

Cold multiproton-transfer reactions in the system $^{86}\text{Kr} + ^{54}\text{Fe}$ below the Coulomb barrier

M. Wilpert, B. Gebauer, W. von Oertzen, Th. Wilpert, E. Stiliaris, and H. G. Bohlen
Hahn-Meitner-Institut Berlin G.m.b.H., Glienicker Strasse 100, D-1000 Berlin 39, Germany

(Received 14 September 1990)

Angular distributions of the one- up to four-proton transfer have been measured in the system $^{86}\text{Kr} + ^{54}\text{Fe}$ at an energy of $E_{\text{lab}} = 291$ MeV. The one- and two-proton-transfer angular distributions are well described by the distorted-wave Born approximation. The three- and four-proton transfers show strong deviations from this approach with contributions which are isotropic. The isotropic component is attributed to reaction processes with a longer time scale. This conjecture is supported by the observed total energy loss of 15–20 MeV, consistent with fission systematics, where strongly deformed and cold fragments are produced. These results are interpreted as the decay of a long-lived two-center system which is stabilized by shell effects.

The study of interactions between nuclei close to the Coulomb barrier has revealed a variety of phenomena, which show that a strong-coupling situation prevails [1]. All degrees of freedom of the individual nuclei (collective excitations, single-particle properties) and of the two-center complex (neck formation, deformed shells) may be relevant in this complex scenario of nucleus-nucleus interactions. If the reactions are studied below the Coulomb barrier, the available kinetic energy, which could possibly be transformed into intrinsic excitation, is only a few MeV (< 20 MeV in our case). Various features known from cold nuclear fission [2], where different valleys of mass fragmentation are determined by the properties of the total system and where pairing properties are manifested in terms of odd-even effects in charge yields, are expected to be observed in corresponding cold multinucleon rearrangement reactions. Properties of these reactions should be linked to the phenomena of superdeformation and hyperdeformation [3] and may have been observed in other studies of rearrangement collisions below the barrier [4,5]. A rich field of nuclear two-center (or molecular) configurations depending on many parameters (total particle number and particle number asymmetry of interacting nuclei, deformation, single-particle properties, angular momentum, etc.) is expected to be hidden in reactions below the Coulomb barrier with low cross sections.

We report here the results of a study of multiproton transfer in the system $^{86}\text{Kr} + ^{54}\text{Fe}$ at an energy below the Coulomb barrier. The measurement was performed with a ^{86}Kr beam at an incident energy of $E_{\text{lab}} = 291$ MeV on a ^{54}Fe target ($180 \mu\text{g}/\text{cm}^2$ on a thin ^{12}C backing). The scattering system was chosen in order to assure Q -value matching of the quasielastic one- to four-proton transfer. Thus, due to the choice of the system, targetlike nuclei which have smaller charges than Fe ($Z = 26$) are favored because their ground-state Q values are more positive than the optimum Q values, Q_{opt} (cf. Table I). For the definition of Q_{opt} see Ref. [5]. Further, due to the properties of the two colliding nuclei, which have closed neutron shells $N = 28$ (^{54}Fe) and $N = 50$ (^{86}Kr), combined transfers of protons and neutrons are less favored.

The experiment was performed at the VICKSI accelerator of the Hahn-Meitner-Institut using a kinematic coincidence setup [6] consisting of two bidimensionally position-sensitive detectors, i.e., a telescope with an angular acceptance of 12.2° in plane and 1.45° out of plane and a low-pressure multiwire chamber (MWC) covering $24^\circ \times 12^\circ$. The distances from the target were 830 and 590 mm, respectively. In the telescope, the ejectiles penetrate a parallel-plate avalanche counter (PPAC) and a proportional counter with resistive wire anode (yielding an in-plane angle resolution of $\delta\theta_L < 0.1^\circ$) and are stopped in an ionization chamber (IC) located in a second gas volume with higher pressure, which allows four successive energy-loss measurements. The out-of-plane angle is derived from the drift time in the IC [6]. The targetlike recoil nuclei were detected in the telescope over the angular range $14^\circ \leq \theta_{\text{lab}} \leq 46^\circ$ with three overlapping angle settings and the associate Kr-like products were detected in the MWC.

Because of the high velocities of the recoil nuclei, an unambiguous Z separation of the targetlike products was achieved with the ΔE - E measurement in the IC over the full range of Q values (cf. Fig. 1). On the other hand, although the time resolution of both the PPAC and the MWC were better than 200 ps, no separation of individual masses was obtained from a time-of-flight (TOF) difference measurement between ejectiles and recoils since the mass lines of neighboring isotopes were overlapping in the TOF vs scattering angle spectra because of the Q -value range included in each line. In addition, the lines were broadened by energy-loss straggling and small-angle straggling of both fragments in the target. Thus, no mass gates were set. But from the widths and the positions of the mass spectra in comparison with the Q -value spectra, it can be concluded that the flux is concentrated predominantly in the transfer of protons with some widening by additional transfer of neutrons. This experimental result is discussed in somewhat more detail below; it confirms the Q -value arguments given above.

Q -value spectra were obtained from two independent methods: at first from the total kinetic energy (TKE) measured with the IC after correction for energy loss

TABLE I. For different reaction channels the ground-state (Q_{00}) and optimum (Q_{opt}) Q values are given. $E_{\text{c.m.}} - E_{\text{Viola}}$ is the maximum available energy in the outgoing channel assuming a fission process for asymmetric mass splits. \bar{Q} and ΔQ are the measured average Q values and their widths, respectively. All values are given in units of MeV.

Transfer	Outgoing channel	Q_{00}	Q_{opt}	$E_{\text{c.m.}} - E_{\text{Viola}}$	$\bar{Q} = Q_{00} - \bar{E}_x$	ΔQ (FWHM)
2p	$^{56}\text{Ni} + ^{84}\text{Se}$	-9.66	1.92	12.2		
1p	$^{55}\text{Co} + ^{85}\text{Br}$	-6.88	1.08	13.1		
1n	$^{54}\text{Fe} + ^{86}\text{Kr}$	0.0	0.0	13.8	0	4
	$^{55}\text{Fe} + ^{85}\text{Kr}$	-0.56				
2n	$^{56}\text{Fe} + ^{84}\text{Kr}$	3.52				
3n	$^{57}\text{Fe} + ^{83}\text{Kr}$	0.65				
4n	$^{58}\text{Fe} + ^{82}\text{Kr}$	3.23				
-1p	$^{53}\text{Mn} + ^{87}\text{Rb}$	-0.23	-1.32	15.0	-2	6
-1p, 1n	$^{54}\text{Mn} + ^{86}\text{Rb}$	-1.22				
-1p, 2n	$^{55}\text{Mn} + ^{85}\text{Rb}$	0.36				
-1p, 3n	$^{56}\text{Mn} + ^{84}\text{Rb}$	-2.86				
-1p, 4n	$^{57}\text{Mn} + ^{83}\text{Rb}$	-2.98				
-2p	$^{52}\text{Cr} + ^{88}\text{Sr}$	3.82	-2.88	16.3	-8	9
-2p, 1n	$^{53}\text{Cr} + ^{87}\text{Sr}$	0.65				
-2p, 2n	$^{54}\text{Cr} + ^{86}\text{Sr}$	1.94				
-3p, -1n	$^{50}\text{V} + ^{90}\text{Y}$	-3.82				
-3p	$^{51}\text{V} + ^{89}\text{Y}$	0.39	-4.67	17.9	-10	12
-3p, 1n	$^{52}\text{V} + ^{88}\text{Y}$	-3.78				
-4p, -2n	$^{48}\text{Ti} + ^{92}\text{Zr}$	-2.57				
-4p, -1n	$^{49}\text{Ti} + ^{91}\text{Zr}$	-3.06				
-4p	$^{50}\text{Ti} + ^{90}\text{Zr}$	0.68	-6.71	19.7	-11	18

both in the target and in the entrance of the telescope, and second from the in-plane angle-angle correlation measurement. In the latter case, the resolution—as inferred from the widths at the high-energy side of the Fe spectra—differs between 4 MeV (20°) and 1.4 MeV (40°) whereas, in the TKE spectra, the resolution is 3.5–4

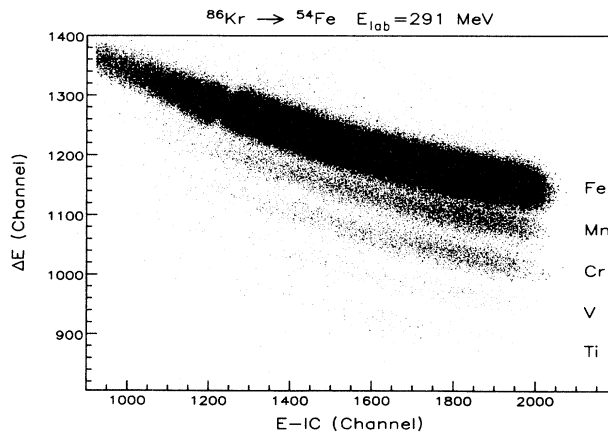


FIG. 1. ΔE - E scatter plot measured with one angle setting of the ionization chamber at 30° ; the angular range of 24° – 36° is covered. The plot documents the unambiguous Z separation obtained for recoil nuclei with $Z = 22$ – 26 .

MeV. With both methods the excitation energy spectra belonging to unresolved isotopes are shifted for different ground-state Q values and overlap in the sum spectra. With the angle-angle correlation measurement, the spectra belonging to different isotopes are also shifted for equal ground-state Q values because of the mass dependence of the kinematics. Both sets of spectra show essentially identical widths and positions for the transfer channels. Selected Q -value spectra measured in the IC, but with the additional restriction of kinematic coincidence, are presented in Fig. 2 together with the TOF spectra belonging to them. In addition, using the out-of-plane angle-angle correlation it was confirmed that no background from nonbinary events was present. In both types of spectra for each element the positions of the ground states are indicated for all isotopes which come close to the proton-transfer channels with respect to ground-state Q value ($\Delta Q = \pm 5$ MeV) and neutron number ($\Delta N = \pm 4$). By detailed inspection of both spectra for each element, the following conclusions can be drawn concerning neutron transfer yields in the spectra (cf. also Table I): For $Z = 26$, visible contributions from neutron transfer to the “elastic” yield (see below) can be excluded as well as for $Z = 25$ (one-proton transfer, $A = 53$) with the exception of the $A = 54$ channel. But the latter spectrum is clearly dominated by the one-proton transfer with an average excitation energy $\bar{E}_x \approx 2$ MeV. For $Z = 24$, the main yield

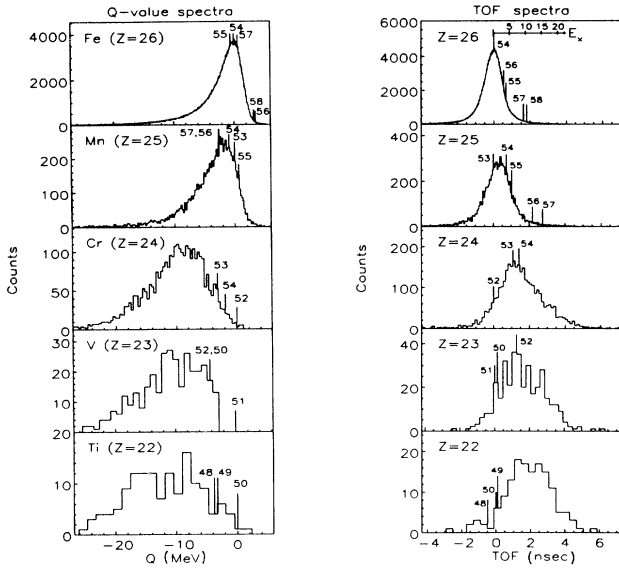


FIG. 2. Q -value spectra measured with the IC at 30° for the elements $Z=22$ – 26 in comparison with the TOF spectra belonging to them. The Q -value spectra were evaluated with the additional restriction of kinematic coincidence in order to exclude nonbinary events. In both types of spectra the positions of the ground states of several isotopes are indicated (see text). In the Q -value spectra the scale is relative to the ground states of the pure proton transfer channels.

clearly corresponds to the two-proton transfer ($A=52$) with $\bar{E}_x \approx 8$ MeV, but contributions from $A=53$ and 54 with smaller excitation energies cannot be excluded. For $Z=23$ the three-proton transfer yield ($A=51$) with $\bar{E}_x \approx 10$ MeV is obscured by the $A=50$ and 52 channels with $\bar{E}_x \approx 7$ MeV. For $Z=22$ the main yield is interpreted as belonging to the four-proton transfer ($A=50$) with $\bar{E}_x \approx 12$ MeV, but contributions from $A=48$ ($\bar{E}_x \approx 8$ MeV), $A=49$ ($\bar{E}_x \approx 9$ MeV) are possible.

Since no separation of individual excited states was achieved in the Q -value spectra (cf. Fig. 2), the inelastic excitations are always contained in the definition of the cross sections for all subsequent transfer steps. No gates were set in the Q -value spectra. This approach for the definition of the quasielastic transfer cross section has been discussed and used in various experiments using heavy ions, where complete separation of the final states was not achieved [7-9]. For larger ΔZ values, the width of the Q -value distribution increases and the average excitation energy increases from about 2 MeV for one-proton transfer to about 12 MeV for four-proton transfer.

Z gates were set as free-form gates in the two-dimensional ΔE - E scatter plots (cf. Fig. 1) to define the cross sections of the “elastic” scattering and of the proton transfers, respectively. A projected spectrum of the element yield (Z spectrum) obtained for one angle setting of the telescope is shown in Fig. 3. As can be seen, the yields for the transfers of even numbers of protons are enhanced with respect to odd proton numbers.

In Fig. 4 we show the angular distributions for the

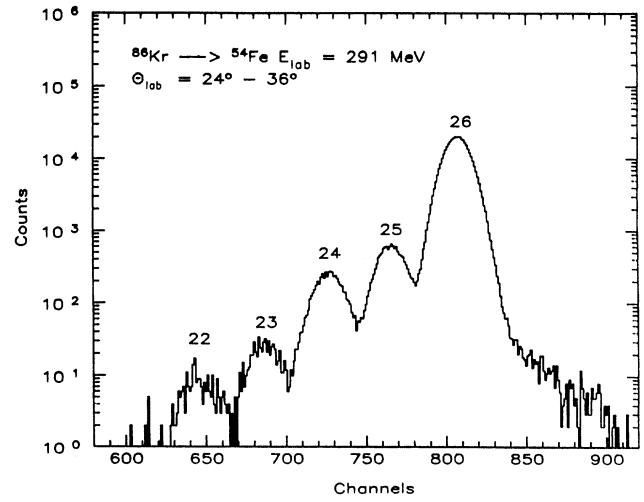


FIG. 3. Projected Z spectrum corresponding to the data of Fig. 1.

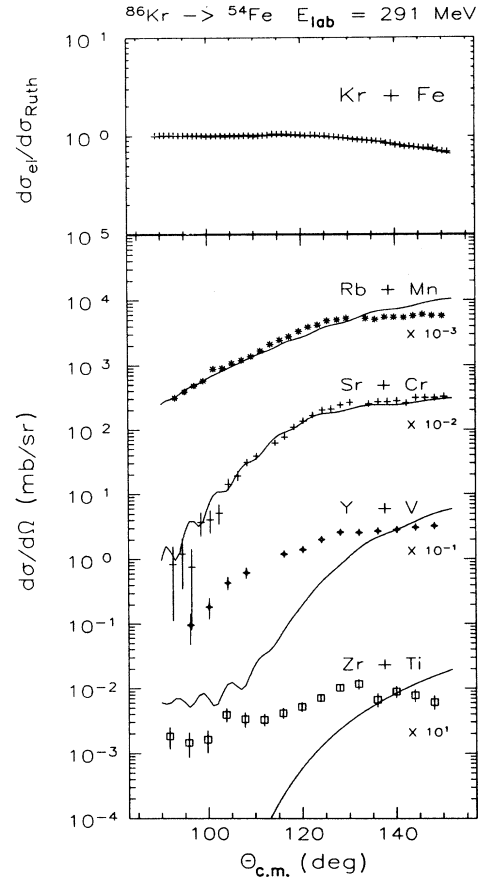


FIG. 4. Angular distributions of the “elastic” scattering and proton-transfer channels containing partially neutron transfers and inelastic excitations (see text). The “elastic” scattering is normalized to the Rutherford cross section. The curves are DWBA calculations (code PTOLEMY) normalized to the data at $\theta_{c.m.} = 140^\circ$. The optical-model parameters used for the calculations are $V=11.5$ MeV, $r_{0V}=1.38$ fm, $a_V=0.5$ fm, $W=0.33$ MeV, $r_{0W}=1.45$ fm, and $a_W=0.4$ fm.

mass- and energy-integrated yields for each element. The “elastic” scattering, which contains inelastic excitations, is shown as $\sigma_{el}/\sigma_{Ruth}$. It deviates only slightly from Coulomb scattering and is used at the smaller CM angles for absolute normalization of the cross sections. Adding back the measured transfer channels almost recovers the original Coulomb scattering cross section (see below). The one- and two-proton transfers show the expected behavior of *quasielastic sub-Coulomb transfer reactions*, whereas the transfer of more than two protons and possibly additional neutrons gives angular distributions which extend to smaller angles. This rather unexpected behavior in the present sub-Coulomb reaction would be typical for deep-inelastic reactions observed at energies above the barrier, where with increasing mass transfer, the energy-loss increases, and a dinuclear complex is formed [10]. The decay of this dinuclear complex gives angular distributions which extend over a large angular range. In the present case, a rotation by at least 40° or negative deflection to angles of 140° and more is necessary to give the cross section for the four-proton transfer.

A consideration concerning the energy loss puts this observation into perspective. We note that the incident energy is below the Coulomb barrier E_C as can be inferred from the shape of the “elastic” angular distribution (cf. Fig. 4). If we define E_C with a parameter $d_0 = 1.35$ fm, with $d_0 = R_{min}/(A_1^{1/3} + A_2^{1/3})$ and $R_{min}(180^\circ)$ being the distance between the centers of mass of both nuclei at $\theta_{c.m.} = 180^\circ$, we obtain $E_C(1.35) = 122$ MeV, which has to be compared with the incident energy of $E_{c.m.} = 112.1$ MeV. Other parametrizations deliver lower values (cf., e.g., Refs. [11] and [12]) of $E_C = 114.0$ MeV and (Ref. [12]) $E_C = 112.8$ MeV, respectively. Using the expression of the Viola systematics for the total kinetic energy of fission fragments [13], extended for an asymmetric mass split [14],

$$\langle TKE \rangle_{as} = (0.1065Z^2/A^{1/3} + 22.1 \text{ MeV})4Z_1Z_2/(Z_1 + Z_2)^2$$

we obtain, for the four-proton transfer channel ($Z_1 = 22$, $Z_2 = 40$), a value of $\langle TKE \rangle_{as} = 93$ MeV. This value is close to the final energy obtained by subtracting from $E_{c.m.} = 112.1$ MeV the energy loss corresponding to a Q value of -15 to -20 MeV observed in this channel with a strong cross section (see Fig. 2). In Table I we give the values of the energy loss expected for the Viola systematics, the values of the average Q values extracted from the experimental spectra for pure proton transfers, and their widths. For the one- to three-proton transfers, the spectra are dominated by the quasielastic process and angular distributions rather reflect this fact. Inspecting the energy spectra in Fig. 2, we find that, for all elements, a component with Q values extending to approximately -20 MeV is observed. If we calculate the minimum distance from the observed relative energy of the final fragments (corresponding to an energy loss of 15 – 20 MeV), we find an overlap parameter of $d_0 = 1.5$ – 1.6 fm. At these distances the nuclear potential between two separated spherical nuclei is too small to affect the

scattering orbit in a perceptible manner. This is so, in particular, for the case of four-proton transfer, where the form factor is very steep. Tests with distorted-wave Born approximation (DWBA) calculations show that a variation of the depths of the spherical real optical-model potential in the entrance and exit channels from 3 to 13 MeV corresponding to potential changes of 120% at $d_0 = 1.55$ fm does not significantly change the shape of the angular distribution in the angular range measured.

Thus, in order to establish nuclear contact, the energy loss must be used mainly in the deformation of one or both fragments leaving only a few MeV for intrinsic excitation. We must therefore conclude that the potential energy of the total system is determined by a cold dinuclear complex where one or both of the two fragments are deformed and that shell effects of the strongly deformed combined system must be assumed to produce an attractive nuclear potential at these large distances. This is in contrast to deep-inelastic reactions (observed above the barrier) where strong nuclear contact already in the entrance channel leads to orbiting and excitation of the fragments [10].

For comparison we quote earlier four-nucleon-transfer measurements below the Coulomb barrier where the reaction was observed to proceed “normally” as a multistep transfer in a multiple first-order transfer approximation [15,16]. The contribution of the long-lived dinuclear complex in these cases, however, may have been missed because of its small cross section. Other measurements of angular distributions of one- and two-neutron transfer using radiochemical methods in collisions of Au on Au and U gave no indication of deviation from Coulomb orbits [17].

For a further discussion it is useful to extract the cross sections of the various channels. From an optical-model fit to the “elastic” scattering we obtain a total reaction cross section of $\sigma_R = 47.5$ mb (excluding the nonobserved neutron transfer to Kr and Fe isotopes and inelastic excitations). Integration of the one- and two-proton transfer yields $\sigma_{1p} = 16.3$ mb and $\sigma_{2p} = 9.4$ mb. The quasielastic transfer part in the three- and four-proton transfer σ_{3p} and σ_{4p} can be obtained by assuming a shape of the angular distribution as expected from a DWBA calculation (see Fig. 4). In a semiclassical picture this is also obtained by a sequential transfer fitted to the data at $\theta_{c.m.} = 140^\circ$. This yields $\sigma_{3p} = 1.1$ mb and $\sigma_{4p} = 0.26$ mb, respectively. With this result we are left with a cross section for a second isotropic component of about 0.15 mb, in both σ_{3p} and σ_{4p} . It was not possible to observe such contributions in the one- and two-proton transfer because of the larger cross sections of the quasielastic part.

The difference between the total reaction cross section σ_R and the sum of the measured transfer cross sections leaves a cross section of approximately 20 mb for fusion. This is in good agreement with, e.g., data from Scarlassara [18] for the systems $^{58}\text{Ni} + ^{90,91,94}\text{Zr}$ and with the results of Ref. [4] for the lowest energy. For equivalent energies with respect to the Coulomb barrier Scarlassara found fusion cross sections of about 6, 12, and 22 mb for the targets ^{90}Zr , ^{91}Zr , and ^{94}Zr , respectively.

The formation of a long-living dinuclear configuration

is most likely supported by shell effects at large deformations as discussed for small and large angular momenta, for example, by Ragnarson and Sheline [19], Åberg [20], and Höller and Åberg [21]. For the present composite system ($Z=62$, $N=78$), a strong shell correction is expected [19–21] for quadrupole and octupole deformations, the latter being connected to mass asymmetry. The role of the mass asymmetry on these shell effects has so far been considered in the context of the potential landscapes of cold fission [2] and recently also in calculations based on a rotating two-center shell model [22].

Finally, we address ourselves to the effect of proton pairing. In both target and projectile nuclei the protons are in open-shell configurations in which pairing is known to produce specific properties, namely, proton-pairing vibrations in ^{54}Fe and a pairing rotational band with the 0^+ ground states of ^{86}Kr , ^{88}Sr , and ^{90}Zr which are populated in this reaction. We apply the semiclassical model [9] and obtain the transfer functions (probabilities) P_{tr} from the definition $P_{\text{tr}} = \sigma_{\text{tr}}(\theta) / \sigma_{\text{el}}(\theta)$ or at a fixed value of R_{min} , the yield of P_{2p} relative to the sequential one-proton transfer given by $(P_{1p})^2$ will appear enhanced by a factor EF, $P_{2p} = \text{EF}(P_{1p})^2$ (as can be seen directly from Fig. 3). We obtain $\text{EF} \approx 10$ for the two-proton transfer. If we use the yield for σ_{3p} and σ_{4p} at $d_0 = 1.55$ fm as representative for the further steps, we find that the four-proton transfer carries the same enhancement $P_{4p} = (P_{2p})^2$ and also $P_{4p} = P_{3p}P_{1p}\text{EF}$. The shape of the $P_{\text{tr}}(d_0)$ functions for the three- and four-proton transfers are, however, now completely changed for larger values of d_0 because of the contributions of the long-lived dinuclear complex as discussed above. The persistence of the pairing enhancement for the second proton pair is an indication that the reaction is a cold

multinucleon transfer and that shell effects of the dinuclear complex can be relevant in the reaction.

In summary, we have observed *cold* multinucleon-transfer reactions between heavy nuclei at an energy below the Coulomb barrier. The results can be understood as a cold rearrangement reaction in which a dinuclear complex is formed. The cross section for the transfer of an even number of protons is enhanced relative to those with odd proton numbers as in cold fission, supporting independently the notion of a cold rearrangement reaction. The nuclear potential at the distances encountered in this reaction is not sufficient to cause strong deviations from the Coulomb scattering orbit. The observation of these deviations cannot be explained by standard nucleus-nucleus potentials. Considerable deformation of the fragments and a potential-energy gain of more than 2% of the Coulomb barrier energy is needed to cause sufficient deviations from Coulomb orbit. This is taken as an indication that the potential energy of the dinuclear complex is influenced by shell effects in the spirit of Ragnarson and Sheline [19], which give an energy gain of several MeV for certain total numbers of protons or neutrons. In the present case the total number of $Z=62$, $N=78$ coincides perfectly with particle numbers, where large shell corrections are predicted for strongly deformed nuclear shapes with mass asymmetry (or octupole deformation) [20,21]. This observation has strong conceptual links to the predicted hyperdeformation [3] and to the properties of the potential surfaces in cold nuclear fission [2]. Studies of cold rearrangement reactions with the precision presented here will, in particular, if combined with modern 4π - γ detector arrays, give interesting insight into shell effects at extreme nuclear deformations and in two-center complexes.

-
- [1] *Proceedings of the Symposium on Heavy Ion Interactions Around the Coulomb Barrier, 1988, Legnano, Italy* (Springer-Verlag, Berlin, 1988).
- [2] J. P. Bocquet and R. Brissot, *Nucl. Phys. A* **502**, 213c (1989).
- [3] J. F. Scharpey-Schaefer, *Nucl. Phys. A* **488**, 127c (1988).
- [4] F. L. H. Wolfs, *Phys. Rev. C* **36**, 1379 (1987).
- [5] F. L. H. Wolfs, R. V. F. Janssens, R. Holzmann, T. L. Khoo, W. C. Ma, and S. J. Sanders, *Phys. Rev. C* **39**, 865 (1989).
- [6] B. Gebauer, D. Fink, P. Goppelt, M. Wilpert, and Th. Wilpert, *Nucl. Instrum. Methods B* **50**, 159 (1990).
- [7] L. J. B. Goldfarb and W. von Oertzen, in *Heavy Ion Collisions*, edited by R. Bock (North-Holland, Amsterdam, 1979), Vol. 1, p. 2A.
- [8] H. Siekmann, B. Gebauer, H. G. Bohlen, H. Kluge, W. von Oertzen, P. Fröbrich, B. Strack, K. D. Hildenbrand, H. Sann, and U. Lynen, *Z. Phys. A* **307**, 113 (1982).
- [9] W. von Oertzen, H. G. Bohlen, B. Gebauer, R. Künkel, F. Pühlhofer, and D. Schüll, *Z. Phys. A* **326**, 463 (1987).
- [10] A. Gobbi and W. Nörenberg, in *Heavy Ion Collisions*, edited by R. Bock (North-Holland, Amsterdam, 1979), Vol. 2, p. 127.
- [11] G. Wirth, W. Bröchle, M. Brügger, Fan WO, K. Sümmerer, F. Funke, J. V. Kratz, M. Lerch, and N. Trautman, *Phys. Lett. B* **177**, 282 (1986).
- [12] R. Bass, *Phys. Rev. Lett.* **39**, 265 (1977).
- [13] V. E. Viola, Jr., *Nucl. Data A* **1**, 391 (1966).
- [14] W. W. Wilcke, J. R. Birkelund, H. J. Wollersheim, A. D. Hoover, J. R. Huizenga, W. U. Schröder, and L. E. Tubbs, *At. Data Nucl. Data Tables* **25**, 389 (1980).
- [15] R. Künkel, W. von Oertzen, B. Gebauer, H. G. Bohlen, H. A. Bösser, B. Kohlmeyer, F. Pühlhofer, and D. Schüll, *Phys. Lett. B* **208**, 355 (1988).
- [16] R. Künkel, W. von Oertzen, H. G. Bohlen, B. Gebauer, H. A. Bösser, B. Kohlmeyer, J. Speer, F. Pühlhofer, and D. Schüll, *Z. Phys. A* **336**, 71 (1990), and references therein.
- [17] F. Funke, Dr. Dissertation, Universität Mainz, 1990 (see GSI report GSI-90-10).
- [18] F. Scarlassara, in *Proceedings of the Symposium on Heavy Ion Interactions Around the Coulomb Barrier, 1988, Legnano, Italy* (Springer-Verlag, Berlin, 1988), p. 79.
- [19] I. Ragnarson and R. K. Sheline, *Phys. Scr.* **29**, 385 (1984).
- [20] S. Åberg, private communication.
- [21] J. Höller and S. Åberg, *Z. Phys. A* **336**, 363 (1990).
- [22] X. Wu, J. A. Maruhn, and W. Greiner, *Z. Phys. A* **334**, 207 (1989).